Pipe Dreams
Optimizing a Snowboard Halfpipe for Maximum Air

Stephen Bidwell, Liam Clegg, Victor Minden

February 14, 2011*

Abstract

The shape of a halfpipe course for snowboarding directly affects the amount of vertical air that a boarder can achieve on it. We used simulations to find the optimal shape for a halfpipe to maximize the potential for vertical air.

We model a halfpipe as a mathematical cylinder defined by 3 variables: w, the width, ϕ, the angle of inclination, and $f(\cdot)$, the shape function representing a vertical cross-section. We model a given run down the pipe by assuming a boarder's trajectory is constrained to the vertical plane containing her initial velocity vector v_0, at angle θ. Finally, we model a snowboarder as a point-mass with a coefficient of friction, μ_k, and a stability function, $\gamma(\cdot)$. The stability function models the effect of the course on her control and influences her trajectory at launch time.

We derive a path integral for the boarder's velocity, taking into account the effects of gravity and friction. By evaluating this integral at the boarder's launch point and combining it with her associated $\gamma(\cdot)$, we develop an expression for her maximum achievable vertical air on an arbitrary halfpipe. We choose $\gamma(\cdot)$ such that finding the ideal halfpipe shape is a non-trivial constrained optimization problem.

In our simulations, we fix representative values for all parameters besides $f(\cdot)$, and use Monte Carlo methods to optimize vertical air across two classes of shape functions: ellipses and sixth-order, even polynomials. Across multiple runs of 400 trials each, our algorithm converged to a unique optimal solution within each shape class. While the halfpipes within each shape class vary substantially in their ability to produce vertical air, the optimal polynomial solution and the optimal elliptic solution do not differ significantly in their maximum air.

1 Introduction

For a snowboarder, getting maximum vertical air on a halfpipe is a constrained optimization problem involving speed and control. More speed at the pipe's upper lip translates to a greater distance traveled through the air, but the boarder must use control to direct her trajectory upwards at launch time. A snowboarder gets most of her speed from two places: the initial speed she drops into one side of the pipe with, and the speed she gains from gravity. The boarder goes down the side of the halfpipe, and the halfpipe is also tilted downhill so that she gains even more speed by traversing the track at an angle.

*Submitted to the 2011 Mathematical Contest in Modeling

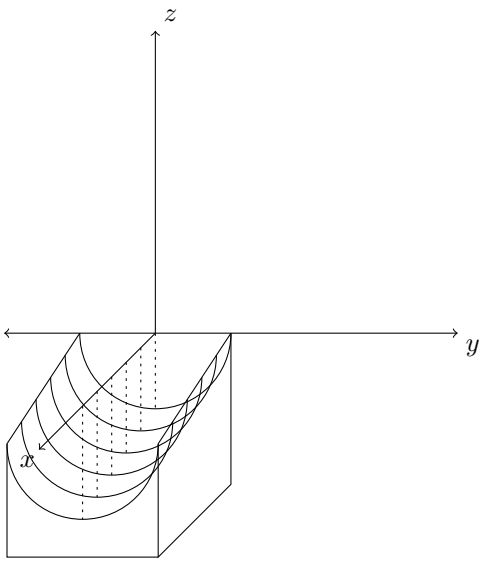

Figure 1: The halfpipe.

2 Model

Our model includes the following variables and parameters:

A halfpipe, ξ, specified by:

- ϕ, the angle of inclination ($^\circ$),
- w, the width (meters),
- $f(\cdot)$, the shape function.

A run, R, specified by:

- θ, the initial angle,
- v_0, the initial velocity.

A snowboarder, SB, specified by:

- m, mass (kilograms),
- μ_k, the coefficient of friction between board and snow,
- $\gamma(\cdot)$, a stability function.

We define our halfpipe in xyz-space, with the positive z-axis pointing up. As shown in Figure 1, the halfpipe is symmetric about the xz-plane, with the tops of its outer edges lying on the y-axis. We make the following assumptions about the halfpipe:

- A halfpipe is smooth and has nonnegative concavity at all points.
- The shape of a halfpipe does not vary along its length.

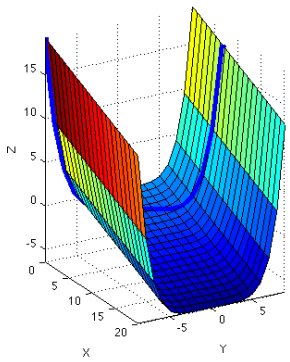

Figure 2: A halfpipe with the snowboarder's path shown in blue.

The first assumption eliminates "halfpipes" with corners, bumps, or discontinuities that make snowboarding on them unrealistic. The second assumption reflects the way real halfpipes are constructed.

With these assumptions, we proceed to model a halfpipe ξ as the mathematical cylinder formed by a smooth function of non-negative concavity $z = f(y)$ (the 'shape' of the halfpipe) and a line in the xz-plane at some angle of inclination ϕ. The halfpipe $\xi = \{\phi, w, f(\cdot)\}$ defines a surface:

$$\left\{(x, y, z) \middle| x \geq 0; -\tfrac{w}{2} \leq y \leq \tfrac{w}{2}; z = f(y) - x \tan\phi\right\}.$$

As the length of a halfpipe has no meaningful impact on the maximum air a boarder can achieve on it, we let the surface goes to infinity in the x-direction.

A snowboarder traversing a halfpipe zig-zags back and forth, gaining speed from the incline of the pipe. We model as a run one zig (or zag), determined by an angle θ and an initial velocity v_0. We measure θ from the y-axis, so that $\theta = 0$ is a run straight across the halfpipe. Initial velocity is in the direction of the initial downward slope of the trajectory. We make one assumption about the run:

- The boarder's trajectory along the halfpipe lies in a plane parallel to the z-axis.

This simplifying assumption is not too far from reality [4, e.g.] The resulting trajectory is shown in Figure 2 (on a decidedly non-optimal halfpipe).

Finally, the snowboarder is determined by a mass m, a coefficient of friction μ_k, and a stability function $\gamma(\cdot)$. Mass is measured in kilograms, and the coefficient of friction is unitless. The stability function determines the way that speed, acceleration, or other factors affect the snowboarder's ability to control the angle of her launch.

For a given ξ, R, and SB, we can compute the expected vertical air Air, measured as maximum vertical distance from the point of take-off on the lip of the pipe. For the current project, we use a representative snowboarder SB^* and a representative run R^*, so that we can simulate the average air achieved by a good snowboarder on each track with the goal

$$\max_{\xi} Air(\xi; SB^*, R^*). \tag{1}$$

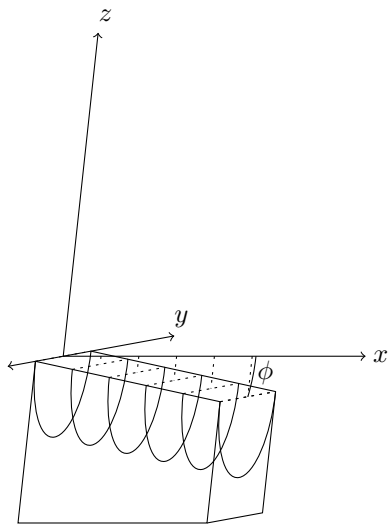

Figure 3: Side view of the half-pipe.

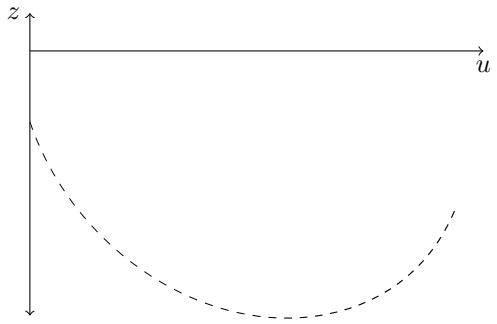

Figure 4: The uz-plane, containing the snowboarder's trajectory

3 Theory

Following our assumption about the boarder's path, we define the u-axis as a line within the xy-plane such that the boarder's trajectory is a two-dimensional curve in the uz-plane, shown in Figure 4. The path of the boarder is then parameterized by

$$\begin{aligned} x(u) &= x_0 + u\sin\theta \\ y(u) &= y_0 + u\cos\theta \\ z(u) &= f(y(u)) - x(u)\tan\phi \\ &= h(x(u), y(u)) \end{aligned} \tag{2}$$

We would like to know the snowboarder's velocity at arbitrary points along her run. To find this, we use the law of total energy, which tells us the that kinetic energy K of the snowboarder at a point b along her path is determined by the gravitational field and the work done by friction along her path, i.e.,

$$K(b) = K(a) + W_g + W_f, \tag{3}$$

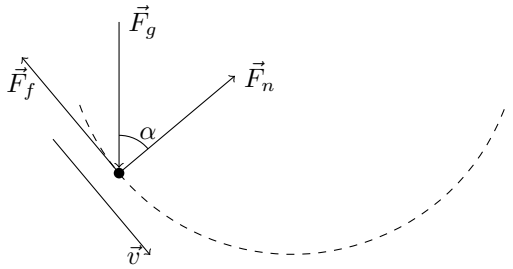

Figure 5: Forces acting on a snowboarder traversing a half-pipe

where a is the initial point of the boarder's run.

Using a as our reference for potential, the initial energy of the boarder is all kinetic, yielding

$$K(a) = \frac{1}{2}m|\vec{v_0}|^2. \tag{4}$$

The next term, W_g, the work done by gravity, is given by

$$W_g = \int_a^b \vec{F_g} \cdot d\vec{s}, \tag{5}$$

with the gravitational field given by

$$\vec{F_g} = \begin{pmatrix} 0 \\ 0 \\ -mg \end{pmatrix}. \tag{6}$$

Since the gravitational field is conservative and acts only along the z-axis, (5) reduces to

$$W_g = mg\left[z(u(b)) - z(u(a))\right],$$

where $u(\cdot)$ is the inverse parametrization of a point in the boarder's path.

Thus the only term that remains to compute is W_f. We know that the work due to friction is given by

$$W_f = \int_a^b \vec{F_f} \cdot d\vec{s}. \tag{7}$$

To compute this integral, we first write $z(u) = h(x, y)$ as the level curve $H(x, y, z) = 0$. At any point on the halfpipe, the gradient of H is then given by

$$\vec{\nabla} H = \begin{pmatrix} \tan\phi \\ -f'(y) \\ 1 \end{pmatrix}. \tag{8}$$

Let $\vec{n}$ be the unit normal vector to H, given by

$$\vec{n} = \frac{\vec{\nabla} H}{|\vec{\nabla} H|}.$$

Then from Newton's Second Law and our knowledge of the system, the forces shown in Figure 5 are given by

$$|\vec{F}_n| = |\vec{F}_g| \cos\alpha = |\vec{F}_g \cdot \vec{n}|$$
$$|\vec{F}_f| = \mu_k |\vec{F}_n|,$$

which gives

$$|\vec{F}_f| = \frac{\mu_k}{|\vec{\nabla} H|} \left| \vec{F}_g \cdot \vec{\nabla} H \right|.$$

Furthermore, (6) and (8) imply

$$\left| \vec{F}_g \cdot \vec{\nabla} H \right| = mg.$$

Thus, (7) becomes

$$W_f = -\mu_k \int_a^b \frac{mg}{|\vec{\nabla} H|} ds,$$

where

$$|\vec{\nabla} H| = \sqrt{\tan^2\phi + (f'(y_0 + u\cos\theta))^2 + 1} = \sqrt{\sec^2\phi + (f'(y_0 + u\cos\theta))^2}$$

and

$$ds = \sqrt{\left(\frac{dx}{du}\right)^2 + \left(\frac{dy}{du}\right)^2 + \left(\frac{dz}{du}\right)^2}.$$

In order to integrate, we compute $\frac{dx}{du}$, $\frac{dy}{du}$, and $\frac{dz}{du}$ from (2), yielding

$$\frac{dx}{du} = \sin\theta,$$
$$\frac{dy}{du} = \cos\theta,$$
$$\frac{dz}{du} = f'(y_0 + u\cos\theta)\cos\theta - \sin\theta\tan\phi.$$

Thus,

$$ds = \sqrt{1 + (f'(y_0 + u\cos\theta)\cos\theta - \sin\theta\tan\phi)^2}\, du.$$

Thence, our integral expands to

$$W_f = -\mu_k mg \int_{u(a)}^{u(b)} \sqrt{\frac{1 + (f'(y_0 + u\cos\theta)\cos\theta - \sin\theta\tan\phi)^2}{\sec^2\phi + (f'(y_0 + u\cos\theta))^2}}\, du. \tag{9}$$

So, plugging (9) into (3), we find the boarder's kinetic energy to be

$$\begin{aligned} K(b) &= K(a) + W_g + W_f \\ &= \frac{1}{2} m |\vec{v_0}|^2 + mg\left[z(u(b)) - z(u(a))\right] \\ &\quad - \mu_k mg \int_{u(a)}^{u(b)} \sqrt{\frac{1 + (f'(y_0 + u\cos\theta)\cos\theta - \sin\theta\tan\phi)^2}{\sec^2\phi + (f'(y_0 + u\cos\theta))^2}}\, du. \end{aligned} \tag{10}$$

Finally, we can use (10) to compute the magnitude of the boarder's velocity at any point, b, along her run

$$|v(b)| = \sqrt{\frac{2K(b)}{m}}. \tag{11}$$

If a and b are the lips on either side of the pipe in our parametrization (2), then

$$u(a) = 0,$$
$$u(b) = \frac{w}{\cos\theta},$$

and we can use these values to compute $|v_{launch}|$ from (11). With this, we can find the Air achieved by any boarder SB on any run R on any halfpipe ξ.

4 Simulations

In order to find the optimal shape $f(\cdot)$ for a halfpipe, in our simulations we fixed $\phi = 18°$ and $W = 18$m, both of which are standard values for real world halfpipes [11]. While our model theoretically allows us to solve for the optimal run R^* on each pipe, for the current project we instead used a representative R^* for all pipes. Based on empirical observation, [18, 14] we fixed the parameters of R^* at $|v_0| = 5\text{m/s}; \theta = 20°$ in all simulations. For a coefficient of friction, we used $\mu_k = 0.01$, which is roughly realistic [9]. The mass of the snowboarder cancels out in our equations, so we do not specify a value for it. Finally, for a stability function, we used

$$\gamma(\xi, R) = \lambda\left(|v_{trough}| - |v_{launch}|\right)\sin\theta, \tag{12}$$

where

- $|v_{trough}|$ is the boarder's speed at the center of the halfpipe ($y = 0$),
- $|v_{launch}|$ is the boarder's speed at the moment she becomes airborne, and
- λ is a normalization constant.

This form for γ reflects the following observations:

- A snowboarder can maintain control better if she accelerates more slowly, by taking a wider angle (i.e. greater θ) down the pipe.
- After accelerating down to the trough of the pipe, a boarder can increase her control more the more speed she gives up while ascending the far side.

We used $\lambda = \frac{1}{3}$ for our simulations to generate realistic Air values.

In addition to the effects of the track on the boarder's stability, the track must obey some absolute limits in order to be safe. We make two assumptions about the safety requirements of the track:

- The track cannot take a boarder above some maximum speed v_{max}.
- The track cannot have curvature at any point greater than some κ_{max}.

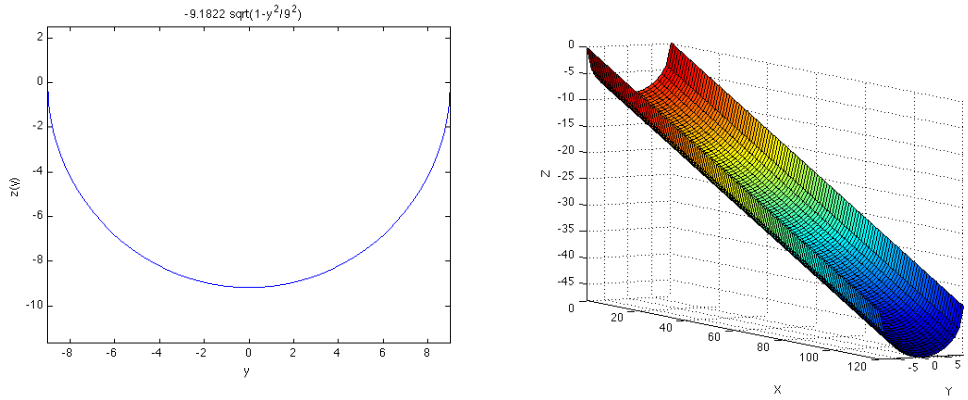

Figure 6: The optimal elliptical halfpipe

We chose $v_{max} = 15\text{m/s}$, and discarded from our consideration those halfpipes which generated speeds above v_{max} on run R^*.

For each track-run pair (ξ, R), we can compute the curvature at any point in the run by

$$\kappa = \frac{|z''(u)|}{(1 + z'(u)^2)^{3/2}}. \tag{13}$$

For each ξ, we computed

$$\kappa(\xi, R^*) = \max_u \kappa(z(u), u; \xi, R^*)$$

numerically and discarded any halfpipes that yielded $\kappa \geq \kappa_{max}$. Based on the physics of snowboards [10, 1], we chose $\kappa_{max} = 1.45\text{m}^{-1}$.

Using (11) and (12), we can compute

$$Air(\xi, R, SB) = \gamma \frac{|v_{launch}|^2}{2g},$$

where g is the gravitational constant. This allows us to estimate (1) by simulation.

Using our model, we tested two different classes of shapes: ellipses and even, sextic polynomials. For each shape class, we ran 10 Monte Carlo simulations of 400 trials each searching the possible parameters of the shape $f(y)$ for the parameters of ξ^*, the pipe that maximized $Air(\xi, R, SB)$.

To verify our methodology, we began by testing an elliptical halfpipe. With w fixed, this leads to a function f with one free parameter b,

$$f(y) = -b\sqrt{1 - \frac{y^2}{(w/2)^2}}. \tag{14}$$

For $w = 18$, our simulations revealed that the optimal elliptical halfpipe, shown in Figure 6, had coefficient

$$\hat{b} = 9.1822 \pm .09\%. \tag{15}$$

This shape yielded

$$Air(\xi^*_{ellipse}; R^*, SB^*) = 2.5877\text{m} \pm .02\%. \tag{16}$$

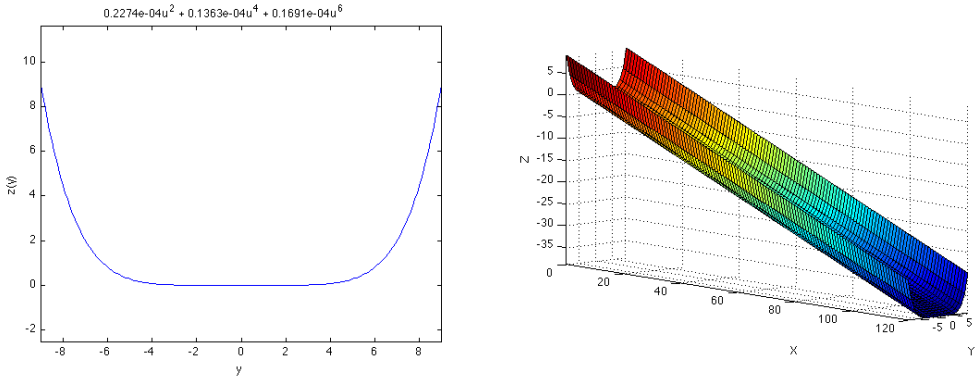

Figure 7: The optimal sixth-order polynomial halfpipe

To solve for a more general curve, we used a sixth-degree polynomial with zero coefficients on all odd terms,

$$f(y) = ay^6 + by^4 + cy^2 + d. \tag{17}$$

In our Monte Carlo simulations, we allowed a, b, and c to vary and chose d such that $f(-w/2) = f(w/2) = 0$. The optimal curves discovered in 10 simulations of 400 trials each had the following coefficient ranges:

$$\begin{aligned} \hat{a} &= 0.00001691 \quad \pm 4.7\% \\ \hat{b} &= 0.00001363 \quad \pm 268\% \\ \hat{c} &= 0.00002674 \quad \pm 99\% \end{aligned} \tag{18}$$

The resulting optimal polynomial halfpipe $\xi^*_{polynomial}$, shown in Figure 7, yielded

$$Air(\xi^*_{polynomial}; R^*, SB*) = 2.5848 \pm .04\% \tag{19}$$

The wide ranges of $\hat{b}$ and $\hat{c}$ in (18) and the narrow range of (19) show that the quartic and quadratic terms in (17) do not play an important role in the shape of the halfpipe $\xi^*_{polynomial}$. The shape of $\xi^*_{polynomial}$ in Figure 7 looks reassuringly similar to real halfpipes [19].

Finally, we wanted to compare our polynomial results to the results of a cycloid, the curve defined parametrically by

$$\begin{aligned} y &= r(t - \sin t) \\ z &= r(1 - \cos t) \end{aligned} \tag{20}$$

for some $r > 0$. Previous research suggests that in some theoretical sense, this is the best shape for a halfpipe [8]. As we fixed w in our simulations, there were no free parameters in our simulation of the cycloidal halfpipe. Since our formulation requires an explicit function $y \mapsto z$, which cannot be obtained from (20), we approximated the appropriate cycloid with a sixth-order polynomial. After computing 100 points on the cycloid for evenly spaced $t \in [0, 2\pi]$, we estimated coefficients in (17) by least squares, yielding

$$f(y) = 0.000009856y^6 - 0.0007106y^4 + .06216y^2 - 5.789. \tag{21}$$

The resulting halfpipe is shown in Figure 8. It yielded

$$Air(\xi_{cycloid}; SB^*, R^*) = 1.6395\text{m},$$

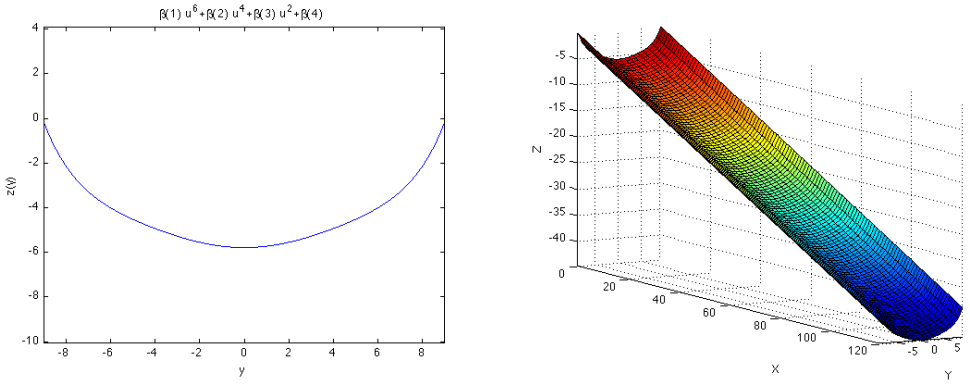

Figure 8: The cycloidal halfpipe

significantly less than the height for the best polynomial pipe. This suggests that while the cycloid has interesting theoretical properties, it is not well-suited to the realities of extreme snowboarding.

5 Discussion

We constructed a model of a halfpipe which allowed us to find the maximum vertical air a snowboarder could achieve on any run. Fixing the parameters of the snowboarder, the run, and the size of the halfpipe, we ran simulations to find the optimal shape.

The optimal shapes yielded by our simulations bear a strong similarity to the shapes of halfpipes used in top-level international competitions [11]. Our optimal elliptical model (15) generated the greatest vertical air of all simulated shapes, though this was not significantly different from that of the optimal sextic pipe (18). Both of these values were significantly greater than the air generated by the cycloidal shape in our model. The polynomial model in particular exhibits many characteristics observed in industrial standard halfpipes, including a wide, flat base with a steep, vertical climb approaching the lip [19].

We fixed all parameters but the shape function in our simulations to reduce the computational complexity of our optimization problem. Faced with a different problem, such as finding the optimal incline for a given shape or the optimal path for a given halfpipe, we could just as easily optimize over other parameters. Given more computational resources, we could compute the optimal run separately on each halfpipe, to account for different riding opportunities afforded by differently shaped pipes.

Perhaps the most unrealistic part of our model is our assumption that the boarder's trajectory lies in a plane parallel to the z-axis. While this assumption greatly simplifies the derivation of (11), it glosses over some of the subtleties of elite halfpipe riding [15]. To allow for the introduction of such subtleties, we could modify our derivation from (7) onward to integrate along a 3-dimensional curve instead of a 2-dimensional one.

Finally, our stability function (12) is highly simplistic. While sufficient to show that our modeling approach works in general, it does not account for nearly all of the factors that go into a snowboarder's ability to get air, such as pumping [12]. However, its role in the model is sufficiently general that it could be modified to include almost any other factor which turns out to be relevant. Furthermore, it could be replaced by a different function

containing the determinants of a goal other than maximizing vertical air, such as maximizing airtime [2] or spin.

References

[1] K. Buffinton, S. Shooter, I. Thorpe, and J. Krywicki, *Laboratory, Computational and Field Studies of Snowboard Dynamics*, Sports Engineering, 6 (2003), pp. 129–137. 10.1007/BF02859890.

[2] J. W. Harding, C. G. Mackintosh, D. T. Martin, A. G. Hahn, and D. A. James, *Automated scoring for elite half-pipe snowboard competition: important sporting development or techno distraction?*, Sports Technology, 1 (2008), pp. 277–290.

[3] J. W. Harding, K. Toohey, D. T. Martin, A. G. Hahn, and D. A. James, *Technoloy And Half-Pipe Snowboard Competition - Insight From Elite-Level Judges*, in The Engineering of Sport 7, Volume 2, Springer, 2008.

[4] S. Koguc, *Snowboard: Mountain Rebels*. http://assets.olympic.org/AFP/JO2010/infographic/en/data/sb/indexen.html, 2009.

[5] S. A. Leduc, *Cracking the GRE Mathematics Subject Test*, New York: The Princeton Review, Inc., 4th ed., 2010.

[6] D. Lind and S. P. Sanders, *The Physics of Skiing: Skiing at the Triple Point*, Woodbury: AIP Press, 1997.

[7] M. J. O'Shea, *Snowboard Jumping, Newton's Second Law and the Force on Landing*, IOPScience, Phys. Educ. 39 335 (2004).

[8] C. Rousseau and Y. Saint-Aubin, *Mathematics and Technology*, New York: Springer, 2008.

[9] T. Sahashi and S. Ichino, *Coefficient of Kinetic Friction of Snow Skis during Turning Descents*, Japanese Journal of Applied Physics, 37 (1998), pp. 720–727.

[10] D. B. Swinson, *Physics and Snowboarding*, The Physics Teacher, 32 (1994), pp. 530–534.

[11] U.S. Ski and Snowboard Association, *2011 USSA Snowboarding Competition Guide*, 2010.

[12] G. Wells, *The Science of Halfpipe Snowboard*. http://www.pmodwrc.ch/pmod.php?topic=tsi/composite/SolarConstant.

[13] Q. Wu and Q. Sun, *A Modified Lift Mechanics Theory for Downhill Skiing and Snowboarding*, in The Engineering of Sport 7, Volume 2, Springer, 2004.

[14] YouTube, *Chevrolet U.S. Snowboard Grand Prix Halfpipe Finals*. http://www.youtube.com/watch?v=aDRfuqrA4Ns, 2005.

[15] ——, *Gretchen Bleiler: Snowboard Spinstress*. http://www.youtube.com/watch?v=t5Ln8t7wWDY, 2008.

[16] ——, *Olympic Snowboarding Halfpipe.* http://www.youtube.com/watch?v=KNXkSwYr4_U, 2008.

[17] ——, *Shaun White 2nd Run Half Pipe Finals Burton NZ Open.* http://www.youtube.com/watch?v=vXjLCBQVnWI, 2009.

[18] ——, *Shaun White's X Games 13 Gold Win In Superpipe.* http://www.youtube.com/watch?v=6UG6vpg-6sU, 2009.

[19] Zaugg America, *Building A Zaugg Half-Pipe.* http://www.zauggamerica.com/resort/pipegroomers/pipe.shtml.